ORIGINAL RESEARCH PAPER

Synthesis, Characterization and Catalytic Activity of Plant-Mediated MgO Nanoparticles Using *Mucuna Pruriens* L. Seed Extract and Their Biological Evaluation

Samira Rahmani-Nezhad [1], Shima Dianat [1], Mina Saeedi [1, 2], Abbas Hadjiakhoondi [1, 3] *

[1] *Medicinal Plants Research Center, Faculty of Pharmacy, Tehran University of Medical Sciences, Tehran, Iran*
[2] *Persian Medicine and Pharmacy Research Center, Tehran University of Medical Sciences, Tehran, Iran*
[3] *Department of Pharmacognosy, Faculty of Pharmacy, Tehran University of Medical Sciences, Tehran, Iran*

Received: 2017-08-09 Accepted: 2017-10-19 Published: 2017-12-20

ABSTRACT
Development of green and efficient procedures for the synthesis of metallic nanoparticles has emerged as a significant topic in the field of nanotechnology. In this respect, using natural resources,especially plant extract has attracted lots of attention; plant extract is a promising alternative to traditional and chemical techniques. The plant *Mucuna pruriens* L. contains high concentration of L-dopa in the seeds; it has been used as a nerve tonic for nervous system disorders including Parkinson's disease. In this work, a rapid and efficient synthesis of stable magnesium oxide nanoparticles (MgO NPs) using aqueous extract of *Mucuna pruriens* seeds were reported. The biologically synthesized MgO NPs were characterized by UV–Visible and Fourier transform infrared (FTIR) spectroscopy as well as X-ray diffraction (XRD), scanning and transmission electron microscopy (SEM and TEM). The potential of MgO nanoparticles in the degeneration of methyl orange (MO) and methylene blue (MB) dyes were assessed in different conditions. The results of these investigations showed that the synthesized MgO NPs have a good catalytic activity in the removal of both dyes. Biological study of biosynthesized MgO NPs showed moderate antibacterial property against four strains of bacteria and a very good antioxidant activity.

Keywords: *Nano MgO; Plant-mediated synthesis; Mucuna pruriens L.; Biological activity; Catalytic property.*

How to cite this article
Rahmani-Nezhad S, Dianat Sh, Saeedi M, Hadjiakhoondi A. Synthesis, Characterization and Catalytic Activity of Plant-Mediated MgO Nanoparticles Using Mucuna Pruriens L. Seed Extract and Their Biological Evaluation. J. Nanoanalysis., 2017; 4(4): 290-298. DOI: 10.22034/jna.2017.540020

INTRODUCTION

Nanobiotechnology has emerged as a multidisciplinary field with significant applications especially in life sciences, health care and modern biomedical researches [1]. In this respect, nanoparticles (NPs) exhibit novel properties due to a large surface area to volume ratio [2]. There are many metal oxides such as MgO, ZnO, CaO, TiO_2 etc., which are known for their widespread uses in gene and drug delivery, biosensors as well as cell and tissue imaging [3-6]. They also have antimicrobial properties and potential for use in diagnostic immunoassays [7-10]. Among various metal oxides, magnesium oxide (MgO) is an interesting basic metal oxide because of versatile applications affected by unique optical, electronic, magnetic,

* Corresponding Author Email: drabbhadji@gmail.com
Tel: +98(21)64121202 Fax +98(21)64121229

thermal, mechanical and chemical properties. MgO is a functional semiconductor metal oxide, which has been widely used in various fields including catalysis, refractory materials, paints, and superconductors [11, 12]. MgO nanoparticles due to high adsorption surface area, a high surface to volume ratio, large numbers of highly reactive edges and destructive sorbents have considerable potential for the adsorption and removal of organic dyes [13, 14].

There are various reports on the synthesis of MgO NPs such as sol–gel, micelle and precipitation processes as well as chemical gas phase deposition, laser vaporization and hydrothermal techniques [15, 16]. It should be noted that most of these methods are expensive and suffer from toxicity and environmental issues, thus using eco-friendly biological systems particularly bio- and plant-mediated synthesis of nanoparticles has attracted a lot of attention [17, 18].

There are different procedures for the synthesis of MgO NPs using *Clitoria ternatea*, [19] *neem leaves*, [20] *Parthenium*, [21] *Brassica oleracea* and *Punica granatum*, [22] *citrus lemon*, [23] *Nephelium lappaceum*, [24] *Artemisia abrotanum*, [25] and *Emblica officinalis* extracts [26]. The efficacy of these synthesized nanoparticles endorses the importance of developing green procedures. *M. pruriens* seeds are rich sources of pharmacologically active secondary metabolites such as L-dopa which are widely used as an antiparkinsonian drug [27]. Also, they have been successfully used for the preparation of gold and silver nanoparticles possessing different size and morphology [28, 29]. Because of the high concentration of L-dopa in the seeds, it can be effective in the synthesis of other nanoparticles. However, there is no report for the green synthesis of MgO NPs using *Mucuna pruriens* L. Seed extract. Herein, we report a green and efficient method for the preparation of MgO NPs using aqueous extract of *Mucuna pruriens* L. seeds that consists of bioactive functional elements which act as reducing and protecting agent in green synthesis of nanoparticles. Moreover, in this study, the potential of biosynthesized MgO NPs in the degeneration of methyl orange and methylene blue dyes were assessed. Finally, the antimicrobial activity of biosynthesized MgO NPs and their in vitro antioxidant activity by DPPH assay were also studied.

MATERIAL AND METHODS

General

All the solvents and reagents used were purchased from Merck and were used without purification. IR spectra were recorded on a Nicolet Magna FT-IR 550 spectrophotometer (KBr disks) in the range 4000–400 cm^{-1}. Absorption measurements were performed on a double beam UV-Vis spectrophotometer in the wavelength range of 200 to 800 nm (160A, Shimadzu, Japan). Nanostructures were characterized using a Holland Philips Xpert X-ray powder diffraction (XRD) diffractometer (CuKα radiation, λ=0.154056 nm), at a scanning speed of 2°/min from 0° to 100°/(2θ). Scanning and transmission electron microscopic (SEM and TEM) were performed on a KYKY-EM3200 and Zeiss-EM10C-100Kv respectively.

Mucuna pruriens L. seeds were purchased from a local market in India and identified at Khomein National Bean Research Station (Figure 1).

Fig. 1. Seeds (*Mucuna pruriens* L.) used for the synthesis of metal nanoparticles.

Preparation of M. pruriens seeds extract

M. pruriens seeds were washed with running tap water and double distilled water respectively for several times and then shade dried for 3–5 days. Dried seeds were powdered in a mixer and used for further investigations.

There are a lot of reports about the L-dopa extraction from *M. pruriens* seeds, which involve the uses of various methods and solvents. Among

these, water extraction has been used here. According to reports, aqueous extracts of *M. pruriens* seeds can have significant amount of L-dopa [30, 31].

A portion of the prepared powder was mixed with some water (10 ml water per 1 gr powder) and kept at 80 °C for 40 min with vigorous magnetic stirring. The mixture was cooled to room temperature, filtered using whatman No. 1 filter paper, and the obtained extract was stored at 4 °C.

Biosynthesis of MgO NPs

Some seed extract was slowly added into some magnesium nitrate hexahydrate ($Mg(NO_3)_2.6H_2O$) solution with the desired concentration (in a proportion: 1:10 v/v). The mixture was stirred at room temperature for 2 h. At first, the formation of magnesium hydroxide ($Mg(OH)_2$) as a precursor for the formation of MgO was observed as the brown color colloidal particles at the bottom of the flask. It was allowed to settle for one day. The mixture was centrifuged at 10000 rpm for 10 min to separate the precipitate. The obtained precipitate washed with deionized water three times to remove impurities. Then, it was dried in the oven at 40°C for at least 12 hand powdered using mortar and pestle. Powdered $Mg(OH)_2$ was calcinated in a muffle furnace at 450°C for 3 h to afford MgO nanoparticles.

Antimicrobial assay of biosynthesized MgO NPs

The biosynthesized MgO NPs using *M. pruriens* seeds extract were evaluated for their antimicrobial activity via disc diffusion method against four of the most pathogenic bacteria, including Gram-negative (Escherichia coli, Pseudomonas aeruginosa) and Gram-positive (Bacillus subtilis, Staphylococcus aureus) ones [32]. 50.0 µL of biosynthesized MgO NPs solution was added to each paper disc (the disc diameter was 6 mm). The paper discs were put on nutritious agar plates that had been previously seeded with inoculum containing indicator microorganisms. After incubation of the plates at 37°C for 16 h, measuring the diameter of growth inhibition zones was done. Antibiotics (gentamicin and chloramphenicol) and DMSO were used as the positive and negative control respectively.

Antioxidant activity of biosynthesized MgO NPs

In this work, the antioxidant activity of biosynthesized MgO NPs using the extract of *M. pruriens* seeds was determined by the decolourization of a DPPH (2, 2-diphenyl-1-picrylhydrazyl) methanol solution during reaction with the solution of biosynthesized MgO NPs. 0.1 ml of the MgO NPs solution (with different concentrations in the range 0.01-5 µg/ml) was added to 0.7 ml of 0.1 mM DPPH solution; changes in the absorbance intensity were measured using the spectrophotometer. After 30 min of shaking the solutions in test tubes, the absorbance was read at the wavelength λ=515 nm. In this method, Rutin hydrates were used as positive control and methanol (95%) as a negative control. The ability to reduce free DPPH radicals was calculated based on the formula:

$Aa=(Ao - Ai/Ao) * 100$ [%]
Aa: antioxidant activity [%],
Ai: average absorbance of the tested solution,
Ao: average absorbance of the DPPH solution.

Catalytic Activity of MgO Nanoparticles

Initially, different solutions at the desired concentrations of dyes (MO and MB) and MgO NPs were prepared. Each test consisted of preparing a 25 mL of dye solution (MO or MB) with the selected initial concentration and different dosage of MgO NPs at room temperature. The prepared solutions were stirred for a predefined time immediately. After the mixing time, the suspension was filtered and used to evaluate the catalytic degradation of dye. The absorbance spectrum of the supernatant was subsequently measured using UV-Vis spectrophotometer at the different wavelength (λmax=464 nm for MO, λmax=664 nm for MB). Percentage of dye degradation was determined using the following formula:

Dye removal efficiency $(\%)=(C_o-C)/C_o * 100$
C_o: initial concentration of dye solution
C: concentration of dye solution after catalytic degradation

The ranges of the experimental variables were as follows: dye concentrations were prepared in the range of 100-800 mg/L for MO and 1-8 mg/L for MB, amount of catalyst (MgO dosage) was in the range of 0.5-3.5 g/L and the mixing time range was 5–120 min. These dosages and conditions were selected according to the results of the protests and also, from the reports of the similar previous studies.

RESULT AND DISCUSSION

Synthesis and characterization

A green and user-friendly method was developed for the synthesis of MgO NPs from aqueous extract of *M. pruriens* seeds. MgO NPs were characterized by UV–Vis and FTIR spectroscopy, as well as X-ray diffraction (XRD), scanning and transmission electron microscopy (SEM and TEM) analysis.

UV-Vis spectroscopy absorption

UV-Vis absorption spectrum of MgO nanoparticles were analyzed in the wavelength range of 200 to 800 nm (Figure 2). The sharp peak at 280 nm indicates the presence of MgO NPs in the reaction media,which is created by reducing of $Mg(NO_3)_2$.

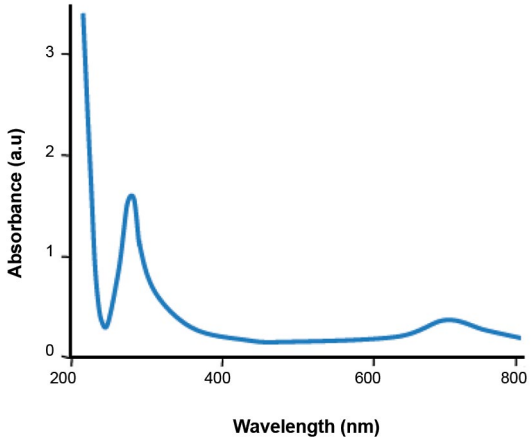

Fig. 2. UV-Vis absorption spectra of MgO NPs.

FTIR Analysis

FT-IR spectroscopy was used to identify the different functional groups of possible bio molecules present in the plant extract which acts as reducing and capping agents of synthesized MgO NPs. As shown in Figure 3, prominent absorption bands were observed at 3421, 1602, 1384, 1351, 1047, 825, and 610 cm^{-1}. The O–H bond vibration is observed as a strong infrared band near 3421 cm^{-1}. The band at 1602 cm^{-1} demonstrates carbonyl group (C=O) vibrations related to amide or typical for the structure of flavonoids which can be found in the *M. pruriens* seeds extract. The band at 1384 cm^{-1} corresponds to C=C stretching of aromatic amine group. The most intense band at 1351 cm^{-1} is related to C–H bending vibrations of aliphatic. The band at 1047 cm^{-1} is characteristic of C-N; this weak band is arisen due to carbonyl stretch in proteins or amino acids. The peak observed around 610 cm^{-1} indicates the presence of metal-oxygen (Mg-O) bending vibration. FTIR spectrum confirmed the presence of bioactive compounds in *M. pruriens* seed extract. These bioactive compounds were presumed to act as reducing and capping agents for MgO NPs. The extract of *M. pruriens* includes flavonoids and high content of L-dopa (amino acid analogue) which demonstrate high antioxidant activity. We believe that, the presence of L-dopa is crucial for the reduction and stabilization of MgO NPs which leads to successfully produce them. In fact, consists of L-dopa in *M. pruriens* seed extract act as reducing, capping and stabilization agent in green synthesis of nanoparticles.

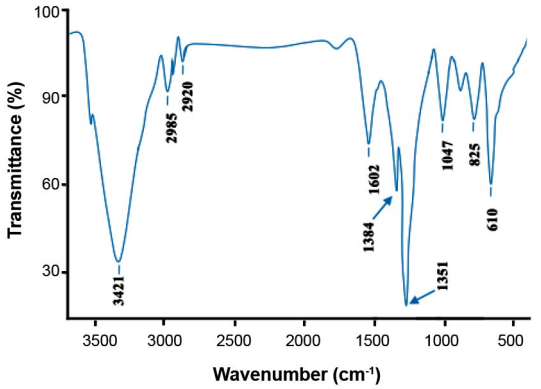

Fig. 3. FTIR spectrum of prepared MgO NPs.

XRD Analysis

Figure 4 shows the X-ray diffraction profile of synthesized MgO NPs. It depicted peaks at 2θ=39.60°, 2θ=42.90°, 2θ=62.86°, 2θ=74.62°, 2θ=78.60° corresponding to (111), (200), (220), (311), (222) planes, respectively. All these diffraction peaks in the XRD pattern of MgO NPs could be indexed as the face centered cubic phase of percales structure (JCPDS No. 39-7746). It confirmed crystalline nature of prepared MgO NPs. The calculated average crystallite size of particles was obtained as 35 nm using Debye Scherrer's formula.

SEM

MgO NPs size, distribution and morphology were analyzed by scanning electron microscopy (SEM) (Figure 5). Most of the particles have spherical shape with an average size of 40-70

nm (with some degree of aggregation) that can be classified as nanoparticles. However, variable parameters such as size, shape and agglomeration of nanoparticles are affected by extract dosage, temperature, and pH.

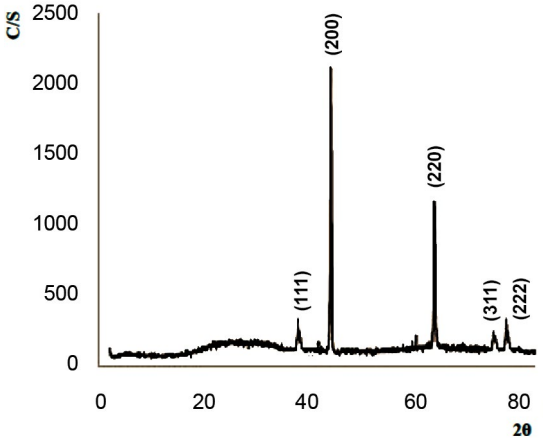

Fig. 4. XRD patterns of synthesized MgO NPs.

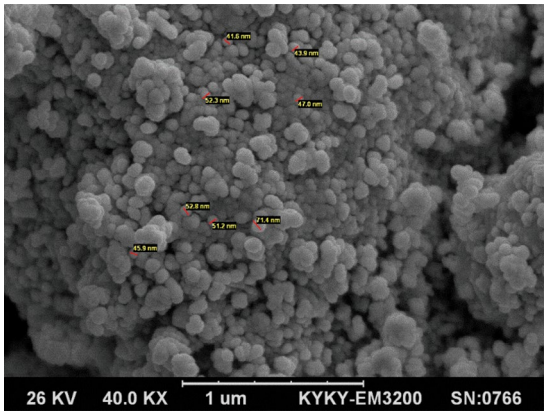

Fig. 5. SEM image of prepared MgO NPs.

TEM Analysis

The size of the synthesized MgO NPs was characterized by using transmission electron microscopy (TEM). TEM has a 1000 times higher resolution than does SEM and is an extremely useful technique to obtain the direct information concerning particle size and the shape of nanoparticles. In this study, it was decided to use both methods in order to measure the size of nanoparticles. Briefly, the sample is suspended in water and coated on a 300 mesh copper grid. The grid is then mounted on the TEM stage for analysis. The TEM image confirmed that the average size of the synthesized MgO NPs was about 50 nm; which most of them had spherical structure (Figure 6). TEM analysis revealed that the synthesized nanoparticles are stable in solution for more than several weeks at room temperature.

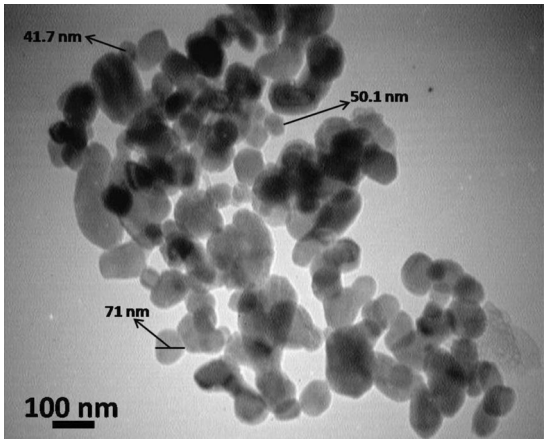

Fig. 6. TEM image of the synthesized MgO nanoparticles.

Catalytic study of biosynthesized MgO NPs

Metallic nanoparticles have very wide uses to catalyze chemical reactions based on the principles of green chemistry. Both MO and MB dyes are an important class of synthetic organic dyes used in the textile industries and are common industrial pollutants. Therefore, finding a simple and environmentally friendly method for the degradation and removal of dyes has gained greater significance among researchers [33, 34]. Metal oxide nanoparticles show enhanced catalytic activity in the degradation of organic dyes. Decomposition of methyl orange (MO) and MB are the often used reaction for testing the catalytic activity of MgO NPs in aqueous solution [35]. In the present work, catalytic activity of MgO NPs was evaluated by monitoring the degradation of MO and MB dyes in aqueous solution using UV-Vis absorption spectroscopy (Figure 7). After adding magnesium oxide nanoparticles to reaction medium, the strong absorption peak that is responsible for methyl orange at λ_{max}=464 nm and Methylene blue at λ_{max}=664 nm was found to decrease meaningfully. This study confirms the catalytic activity of green

synthesized MgO NPs, which may be applied in the degradation of organic dyes.

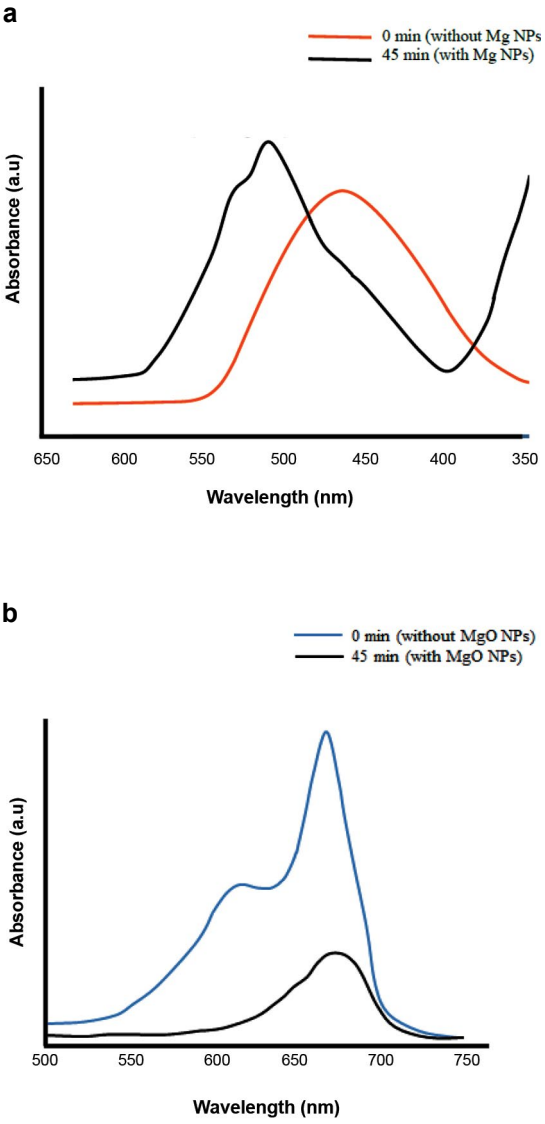

Fig. 7. Absorption spectra of MO (a) and MB (b) reduction by MgO nanoparticles.

Effect of MgO dosage, dye dosage and contact time

Effect of MgO nanoparticle dosage on MO and MB dyes removal efficiency at the constant dye concentrations and constant time (45 min) was evaluated. As seen in Figure 8, when MgO dosage increased, dye removal efficiency increased. These can be attributed to the increase of the available adsorption sites with the increase of MgO dose.

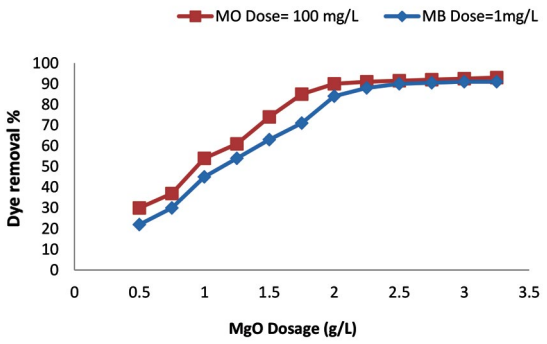

Fig. 8. Effect of MgO dose on the MO and MB removal percentage.

In Figure 9, dyes removal (%) vs. dyes concentration at the constant concentration of MgO NPs (2.5 g/L) and constant time (45 min) are shown. As observed, the dye removal efficiency increased steadily as initial dye concentration increased from 100 to 300 mg/L for MO and 1 to 2 mg/L for MB, and then it decreased sharply with increasing dye concentration, which may be caused by decreasing the number of remaining adsorption sites. Also, at higher dye concentrations (greater than about 400 mg/L for MO and 4 mg/L for MB), removal efficiency was more steadily decreased, which may be related to desorption phenomena occurring [14]. It shows that nanoparticles at the optimum concentration of 2.5 g/L, couldn't adsorb dyes above 400 mg/L for MO and 4 mg/L for MB.

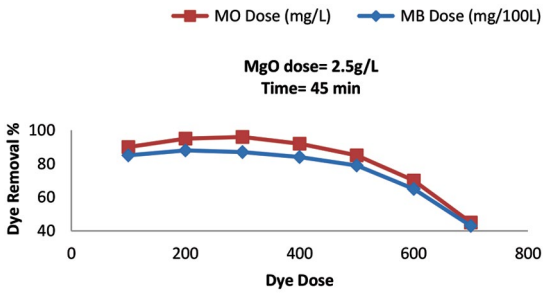

Fig. 9. Effect of MO and MB concentration on removal efficiency.

One of the most important parameters in dye removal processes is contact time. According to Figure 10, by increasing time, dye removal efficiency was increased. This increase was sharp in the first 15-20 min of contact time respectively for MO and MB, and then was gradually flattened out. Therefore, it seems that the best effective

adsorption time can be considered as about 15-20 min and to obtain 90% adsorption efficiency 40-60 minutes is required.

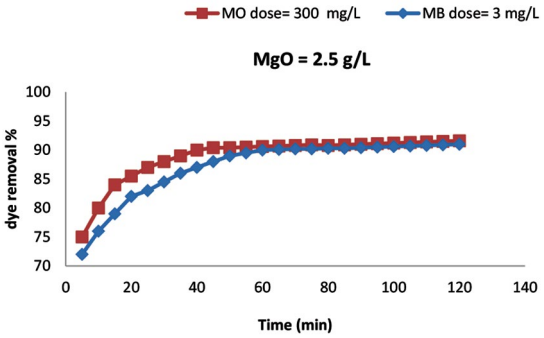

Fig. 10. Effect of contact time on the dye removal efficiency.

Biological study of biosynthesized MgO NPs

Antimicrobial evaluation of biosynthesized MgO NPs

In the present study, the disc diffusion method was used for determining the antimicrobial activity of biosynthesized *MgO NPs* (Table 1). Biosynthesized *MgO NPs* showed a moderate antimicrobial activity against both Gram-positive and Gram-negative bacteria in comparison with gentamicin and chloramphenicol as standard antibiotics. The antimicrobial property of MgO NPs was proved from the zone of inhibition. Despite the lack of clarity in the antibacterial mechanism of MgO nanoparticles, several mechanisms have been suggested in this regard. One of the most important proposed mechanisms is the formation of ROS and the interaction of nanoparticles with bacteria, which causes damage to bacterial cells and subsequently an alkaline effect [36].

Antioxidant activity of biosynthesized MgO NPs

DPPH radical scavenging assay is the most common assay which is used for preliminary screening of the biosynthesized MgO NPs for determining their antioxidant activity. In the DPPH method, antioxidants present in the tested sample reduce the stable nitrogen radical in 2, 2-diphenyl-1-picrylhydrazyl (DPPH), causing the decrease in absorbance measured at the wavelength of 515 nm. After adding antioxidants to DPPH solution, the color of this solution changes, the level of this change shows the amount of free radical scavenging properties of antioxidants [37]. This study investigated the antioxidant activity of the *Mucuna pruriens* seed extract itself and the synthesized MgO NPs using this extract (Table 2). Antioxidant activity determined by calculating the IC_{50} parameter. The results revealed that the biosynthesized nanoparticles were more effective DPPH scavenging agents then the *Mucuna pruriens* seed extract itself.

Table 1. Antimicrobial activity of biosynthesized MgO NPs[a]

Bactria strain	MgO NPs (50.0 µl)	Standard antibiotic	
		Gentamicin (10 µg/disc)	chloramphenicol (30 µg/disc)
E.coli	13.2 ± 1.1	20.8 ± 0.7	21.1 ± 1.1
P.aeruginosa	6.1 ± 0.4	9.4 ± 1.3	-
S.aureue	10.2 ± 1.2	15.4 ± 0.2	21.3 ± 1.5
B.subtilis	15.1 ± 1.5	24.1 ± 0.6	21.9 ± 0.3

[a]Using aqueous $(Mg(NO_3)_2.6H_2O)$ (100 ml, 1 mM) and *Mucuna pruriens* L. seed extract (10 ml, 100 mg ml^{-1}).
Positive controls: Gentamicin and chloramphenicol, negative control: DMSO.

Table 2. antioxidant activity of *Mucuna pruriens* seed extract and Biosynthesized MgO NPs

Test sample	IC_{50} (µg/ml)
Mucuna pruriens extract	9.2±0.15
Biosynthesized MgO NPs	5.34±0.11
IC_{50}: inhibitory concentration 50%	

CONCLUSION

This work described a plant-mediated synthesis of MgO NPs using aqueous extract of *Mucuna pruriens* seeds. *M. pruriens* seeds have a high concentration of L-dopa; this is the reason that, this plant has been studied for its possible use in Parkinson's disease. We proposed an ecofriendly method for the synthesis of MgO nanoparticles using this plant. The obtained nanoparticles were stable for several weeks and the rate formation of them was extremely rapid and higher or comparable to the rate of MgO nanoparticles synthesis by chemical methods or other plant sources. It seems that L-dopa component was mainly responsible for the reduction and the stabilization of the nanoparticles. Characterizations of the biosynthesized nanostructures were performed by UV–Vis, FTIR, XRD, as well as SEM and TEM. It was also investigated the efficiency of prepared nanoparticles on MO and MB dye removal. Time, MgO and dyes dosage were the variable parameters in this work. Results of this investigation showed that the best performance was obtained when the optimum dose of MgO nanoparticles was 2.5 g/L, MO and MB dose were 300 and 2 mg/L with the contact time of 15-20 min. The biosynthesized MgO NPs also showed strong antioxidant property and moderate antimicrobial activity against both Gram-positive and Gram-negative bacteria; hence they can have potential applications in biomedical fields.

ACKNOWLEDGMENT

Authors acknowledge financial support from Reseach Consil of Tehran University Medical Sciences and Iran National Science Foundation (INSF).

CONFLICT OF INTEREST

The authors declare that there is no conflict of interests regarding the publication of this manuscript.

REFERENCES

1. W.J. Parak, D. Gerion, T. Pellegrino, D. Zanchet, C. Micheel, C.S. Williams, R. Boudreau, M.A. Le Gros, C.A. Larabell and P.A. Alivisatos, Nanotechnology. 14, 15 (2003).
2. P. Mohanpuria, N.K. Rana and S.K. Yadav, J. Nanopart. Res., 10, 507 (2008).
3. P.M. Tiwari, K. Vig, V.A. Dennis and S.R. Singh, Nanomaterials. 1, 31 (2011).
4. J.M. Nam, C.S. Thaxton and C.A. Mirkin, Science. 301, 1884 (2003).
5. S. Parveen, R. Misra and S.K. Sahoo, Nanomedicine. 8, 147 (2012).
6. H. Kashif and H. Touseef, South Indian J. Biol. Sci., 1, 128 (2015).
7. S.S. Zinjarde, Chronic Young Sci., 3, 74 (2012).
8. K. Bahrami, P. Nazari, M. Nabavi, M. Golkar, A. Almasirad and A.R. Shahverdi, Nanomed. J., 1, 155 (2014).
9. S.M. Dizaj, A. Mennati, S. Jafari, K. Khezri and K. Adibkia, Adv. Pharm. Bull., 5, 19 (2015).
10. J.A. Lemire, J.J. Harrison and R.J. Turner, Nature Rev. Microbiol., 11, 371 (2013).
11. J.K. Salem, I.M. El-Nahhal, T.M. Hammad, S. Kuhn, S.A. Sharekh, M. El-Askalani and R. Hempelmann, Chem. Phys. Lett., 636, 26 (2015).
12. G.I. Almerindo, L.F. Probst, C.E. Campos, R. M. De Almeida, S.M. Meneghetti, M.R. Meneghetti, J.-M. Clacens and H.V. Fajardo, J. Power Sources. 196, 8057 (2011).
13. G. Moussavi and M. Mahmoudi, J. Hazard. Mater., 168, 806 (2009).
14. R. Wanchanthuek and W. Nunrung, J. Environ. Sci. Technol. 4, 534 (2011).
15. K.V. Rao and C.S. Sunandana, J. Mater. Sci., 43, 146 (2008).
16. S. Balamurugan, L. Ashna and P. Parthiban, J. Nanotechnol., 1 (2014).
17. (a) Nanoparticle Technology Handbook, M. Hosokawa, K. Nogi, M. Naito and T. Yokoyama. (2007) (b) K.S. Kavitha, B. Syed, D. Rakshith, H.U. Kavitha, H.C. Yashwantha Rao, B.P. Harini and S. Satish, Int. Res. J. Biol. Sci., 2, 66 (2013).
18. (a) J. Jeevanandam, Y. S. Cha and M.K. Danquah. NewJ. Chem., 41, 2800 (2017) (b) K. Jhansi, N. Jayarambabu, K. Paul Reddy, N. Manohar Reddy, R. Padma Suvarna, K. Venkateswara Rao, V. Ramesh Kumar, and V. Rajendar. 3 Biotech. 7, 263 (2017).
19. N. John Sushma, D. Prathyusha, G. Swathi, T. Madhavi, B. Deva Prasad Raju, K. Mallikarjuna and K. Hak-Sung, Appl. Nanosci., 6, 437 (2016).
20. S.K. Moorthy, C.H. Ashok, K. Venkateswara Rao and C. Viswanathan, Mater. Today Proc., 2, 4360 (2015).
21. D. Kumar, L.S.R. Yadav, K. Lingaraju, K. Manjunath, D. Suresh, D. Prasad, AIP Conf. Proc., 1665, 050145 (2015)
22. P. Sugirtha R., Divya, R. Yedhukrishnan, K.S. Suganthi, N. Anusha, V. Ponnusami and K.S. Rajan, Asian J. Chem., 27, 2513 (2015).
23. A.M. Awwad and A.L. Ahmad, Arab J. Phys. Chem., 1, 66 (2014).
24. J. Suresh, R. Yuvakkumar, M. Sundrarajan and S.I. Hong, Adv. Mater. Res., 952, 141 (2014).
25. R. Dobrucka, Iran J. Sci. Technol. Trans. Sci., (in press).
26. K. Ramanujam and M. Sundrarajan, J. Photochem. Photobiol., 141, 296 (2014).
27. P. Kulhalli, Parkinson's disease therapy- an overview, Heritage Heal., P. 29-30 (1999).
28. S. Arulkumar and M. Sabesan, Pharmacognosy Res., 2, 233 (2010).
29. S. Arulkumar and M. Sabesan, Int. J. Res. Pharm. Sci., 1, 417 (2016).
30. M. Laxminarain and W. Hildebert, Indian J. Biochem. Biophys., 44. 56 (2007)
31. A.A. Teixeira, E.C. Rich and N.J. Szabo, Trop. Subtrop. Agroecosyst., 1, 159 (2003).

32. S. Asghari, R. Baharfar, M. Alimi, M. Ahmadipour and M. Mohseni, Monatsh. Chem., 145, 1337 (2014).

33. B. Reddy Ganapuram, M. Alle, R. Dadigala, A. Dasari, V. Maragoni and V. Guttena, Int. Nano Lett., 5, 215 (2015).

34. S. Ashokkumar, S. Ravi, V. Kathiravan and S. Velmurugan, Spectrochim. Acta A., 121, 88 (2014).

35. (a) M. R. Rezaii Mofrad, G.R. Mostafaii, R. Nemati, H. Akbari and N. Hakimi, Desalin. Water Treat., 57, 8330 (2016) (b) Z. Raheem and A. M. Hameed, Int. J. Basic Appl. Sci., 4, 81 (2015) (c) K. Mageshwari and R. Sathyamoorthy, Trans. Ind. Inst. Met., 65, 49 (2012) (d) A. Sierra-Fernandez, S.C. De la Rosa-García, L.S. Gomez-Villalba, S. Gómez-Cornelio, M.E. Rabanal, R. Fort and P. Quintana, ACS Appl. Mater. Interfaces. 9, 24873 (2017).

36. (a) Z.X. Tang and B.F. Lv, Braz. J. Chem. Eng., 31, 591 (2014) (b) L. Huang, D.Q. Li, Y. J. Lin, D.G. Evans and X. Duan, Chin. Sci. Bull., 50, 514 (2005) (c) L. Huang, D.Q. Li, Y.J. Lin, M. Wei, D.G. Evans and X. Duan, J. Inorg. Biochem., 99, 986 (2005) (d) S. Makhluf, R. Dror, Y. Nitzan, Y. Abramovich, R. Jelinek and A. Gedanken, Adv. Funct. Mater., 15, 1708 (2005) (e) P.K. Stoimenov, R.L. Klinger, G.L. Marchin and K.J. Klabunde, Langmuir, 18, 6679 (2002) (f) O. Yamamoto, T. Fukuda, M. Kimata, J. Sawai and T. Sasamoto, J. Ceram. Soc .Jpn., 109, 363 (2001).

37. (a) W. Brand-Williams, M.E. Cuvelier and C. Berset, LWT-Food Sci. Technol., 28, 25 (1995) (b) V. Bondet, W. Brand-Williams and C. Lebensmitt, Wissenschaft Technologie Food Sci. Technol., 30, 609 (1997) (c) M. Gangwar, M. Kumar Gautam, A. Kumar Sharma, Y. B. Tripathi, R. K. Goel and G. Nath, Sci. World J., 12 (2014).